International Journal of Pharmaceutics 380 (2009) 189–200

Contents lists available at ScienceDirect

International Journal of Pharmaceutics

journal homepage: www.elsevier.com/locate/ijpharm

Pharmaceutical nanotechnology

Ethylendiamine core PAMAM dendrimers/siRNA complexes as *in vitro* silencing agents

A.P. Perez, E.L. Romero, M.J. Morilla*

Programa de Nanomedicinas (PNM), Departamento de Ciencia y Tecnología, Universidad Nacional de Quilmes, Roque Saenz Peña 352, Bernal B1876BXD, Buenos Aires, Argentina

ARTICLE INFO

Article history:
Received 10 January 2009
Received in revised form 24 June 2009
Accepted 25 June 2009
Available online 3 July 2009

Keywords:
Dendrimers
siRNA
Size

ABSTRACT

We have screened the formation of complexes between ethylendiamine (EDA) core polyamidoamine (PAMAM) dendrimers (D) and a short interfering RNA (siRNA) as a function of three variables: the ionic strength of the medium (lacking or containing 150 mM NaCl), the D generation (G4, G5, G6 and G7) and the N/P ratio (nitrogen amines in D/phosphate in siRNA).

It was observed that all D formed complexes with siRNA, being the size of the complexes strictly dependent on the ionic strength of the media. The strong electrostatic interactions occurring in NaCl lacking medium made siRNA–D complexes (siRNA–D) smaller than those obtained in NaCl containing medium (30–130 nm, +25 mV zeta potential vs. several μm-800 nm, 0 zeta potential, respectively). Not surprisingly, both the uptake and inhibition of EGFP expression in cell culture, resulted dependent on siRNA–D size. siRNA–D prepared in NaCl containing medium were poorly captured and presented a basal activity on phagocytic (J-774-EGFP) cells, being inactive on non-phagocytic cells (T98G-EGFP). However, the smaller siRNA–D prepared in NaCl lacking medium were massively captured, exhibiting the highest inhibition of EGFP expression at 50 nM siRNA (non-cytotoxic concentration).

Remarkably, siRNA-G7 produced the highest inhibition of EGFP expression both in T98G-EGFP (35%) and J-774-EGFP (45%) cells, in spite of inducing a lower protection of siRNA against RNase A degradation.

Taken together, our results showed that modifying the chemical structure of D is not the only way of achieving siRNA–D suitable for silencing activity. The simple use of a low ionic strength preparation media has been critical to get small siRNA–D that could be captured by cells and in particular, siRNA-G7 but not those formed by lower generation D, possessed structural constraints other than size that could favor its silencing activity.

1. Introduction

Short (20–25 base pairs-bp) interfering double strain RNAs (siRNA) are the effectors molecules of a genetic inhibition mechanism known as RNA interference (RNAi). Once inside the cells, siRNA molecules assemble to an endonuclease-containing complex, the RNA-induced silencing complexes (RISC), by which one strand of the duplex is cleaved and discarded. The remaining antisense strand guides the RISC to complementary RNA molecules, where they cleave and destroy the target RNA (Elbashir et al., 2001; Eccleston and Eggleston, 2004; Riddihough, 2005).

Nowadays however, the envisioned potential therapeutic applications of siRNA for the treatment of cancer (Devi, 2006) and cardiovascular diseases (Quarck and Holvoet, 2004), are spoiled by the limitations for *in vivo* siRNA application, such as rapid degradation in blood (Sioud, 2005), fast hepatic and renal clearance (Paroo and Corey, 2004) and low cellular membrane permeability (Zhang et al., 2007). The development of new delivery systems could overcome those barriers, protecting siRNA from rapid degradation and elimination, and by providing targeted tissular, cellular and subcellular delivery (Fattal and Bochot, 2008).

Up to now, the most widely studied delivery systems for nucleic acids rely on the formation of electrostatic complexes between negatively charged nucleic acids and cationic liposomes or polymeric nanoparticles (Zhang et al., 2007). However, in spite of sharing a negatively charged phosphodiester backbone at physiological pH, molecular weight and topography of siRNA strongly differ from that of plasmidic DNA (pDNA) (Gary et al., 2007). Since typical 21 bp siRNA behaves as rigid rod that, opposite to pDNA, is not likely to further condense, siRNA forms weaker complexes with cationic polymers, the complexes being more difficult to be formed. It has been suggested that disordered interactions between siRNA and cationic agents may result in incomplete encapsulation and/or undesirably large complexes (Spagnou et al., 2004).

In the last years, a number of authors have explored the use of a new type of synthetic polymer, the cationic dendrimers, for pDNA or

* Corresponding author. Tel.: +54 1143657100; fax: +54 1143657132.
E-mail address: jmorilla@unq.edu.ar (M.J. Morilla).

0378-5173/$ – see front matter © 2009 Elsevier B.V. All rights reserved.
doi:10.1016/j.ijpharm.2009.06.035

antisense oligonucleotides (AS-ODN) delivery *in vitro* (Haensler and Szoka, 1993; Bielinska et al., 1996; Kukowska-Latallo et al., 1996; Tang et al., 1996; Yoo et al., 1999; Dufes et al., 2005). Dendrimers (D) are unique polymers with a central core and branched surface, with controllable nanoscale size, high monodispersity, controlled number of surface groups, high area/volume ratio and absence of *entanglement* or sticky interactions. Largest D are able to adsorb to and disrupt plasma membranes; also once endocitosed or phagocitosed, cationic D are able to reach cytoplasm upon endosomal disruption (Svenson and Tomalia, 2005).

Bielinska et al. in 1996 showed for the first time specific and dose dependent inhibition of luciferase expression using ethylendiamine (EDA) core polyamidoamine (PAMAM) generation 5 and 7 D and AS-ODN at pM concentrations, while other transfection regents required μM or nM AS-ODN concentrations (Bielinska et al., 1996). Later in 1999, Yoo et al. (1999) observed that only AS-ODN-PAMAM, and not Lipofectamine2000, remained active in the presence of serum. Finally it was found that modifying D structure by conjugation with hydrophobic molecules such as the fluorescent dye Oregon green 488 and cholesterol, enhanced the delivery of AS-ODN by dendrimers (Yoo and Juliano, 2000; Dung et al., 2008).

Currently however, controversial experimental evidence has discarded the use of EDA core PAMAM D to form complexes with siRNA, because of their unsuitable structure. Hence, in this work we have re-visited the use of different size EDA core PAMAM D to form complexes with siRNA, with emphasis on the influence of ionic strength of the preparation media on size, relative binding affinity and zeta potential of complexes, and its relation to their cellular uptake and silencing activity.

2. Materials and methods

2.1. Materials

EDA core polyamidoamine D (PAMAM) of generation 4 (G4, Mw = 14215.17, 64 amine end groups), generation 5 (G5, Mw = 28824.81, 128 amine end groups), generation 6 (G6, Mw = 58046.11, 256 amine end groups) and generation 7 (G7, Mw = 116488.71, 512 amine end groups) were purchased from Sigma–Aldrich, Argentina. Sodium 3-(4,5-dimethythiazole-2-yl)-2,5-diphenyltetrazolium bromide (MTT), RNase A from bovine pancreas, colominic acid (poly[2,8-(N-acetylneuraminic acid sodium salt)]), diethylaminoethyl-dextran (DEAE-Dextran) and diethyl pyrocarbonate (DEPC) were also from Sigma–Aldrich, Argentina. Foetal calf serum, antibiotic/antimycotic solution, glutamine and trypsina/EDTA were acquired from PAA Laboratories GmbH, Austria. Ethidium bromide was purchased from Plusone, Sweden. Chitosan was supplied by Novamatrix, Norway.

The plasmid encoding enhance green fluorescence protein pEGFP-C1 was kindly provided by Dr. Marcos Bilen (Universidad Nacional de Quilmes, Buenos Aires, Argentina). T98G cells and T98G cells stably expressing EGFP (T98G-EGFP) were kindly provided by Dr. David Silvestre (Universidad Nacional de Córdoba, Córdoba, Argentina). Cy3-labeled siRNA was from Genbiotech, Argentina. Lipofectamine2000™, MEM with non-essential amino acids and the antibiotic G418 (geneticin) were purchased GIBCO, Argentina.

EGFP siRNA sense sequence 5′-GCACGACUUCUUCAAGUCCdTdT-3′ and 5′-GGACUUGAAGAAGUCGUGCdTdT-3′(antisense) obtained from Invitrogen Argentina was used for structural studies, while Silencer® EGFP siRNA from Ambion Argentina, was used for inhibition of EGFP expression studies.

All other chemicals and reagents were of analytical grade from ICN Biomedicals, Argentina. All solutions were treated with 0.1% DEPC.

2.2. Analysis of siRNA–dendrimer complex formation and characterization

2.2.1. Ethidium bromide (EtBr) displacement assay

First, the fluorescence of 16.7 μM EtBr [10 mM Tris–HCl pH 7.5 (Tris–HCl buffer)] either containing (*c*) or lacking (*l*) 150 mM NaCl (λ_{ex}: 506 nm and λ_{em}: 590 nm) was recorded on a LS55 fluorescence spectrometer (PerkinElmer, Boston, MA). Upon adding 0.69 nmol of siRNA (1:50 siRNA:EtBr molar ratio), the siRNA:EtBr solutions were titrated by incremental additions of D, up to a maximum volume of 1% (v/v) in order to minimize the dilution effects. After 5 min, each fluorescence was recorded and the relative fluorescence was calculated as follows: $F_r = (F_{obs} - F_{EtBr})/(F_o - F_{EtBr})$, where F_r is the relative fluorescence, F_{obs} is the recorded fluorescence, F_{EtBr} is the fluorescence of the EtBr solution, and F_o is the fluorescence of the siRNA:EtBr solution in the absence of D.

Similarly, 16.7 μM EtBr was titrated by incremental additions of siRNA solution (20 nmol/ml) up to a total of 0.69 nmol siRNA. After each siRNA addition, F_r was calculated as described above, but now F_{obs} is the recorded fluorescence after each siRNA addition and F_o is the fluorescence upon the last siRNA addition corresponding to a total amount of 0.69 nmol siRNA.

2.2.2. Polyacrylamide gel electrophoresis studies

Different amounts of D were mixed with 2 μl of 100 μM siRNA, up to variable N/P ratios (±charge ratios = [nitrogen amines in D/phosphate in siRNA]), considering that 30 μg of G4, G5, G6 and G7 D contain nearly 0.13 μmol of amine nitrogen or positive charges and 35.2 μg of siRNA contain 0.1 μmol of phosphate or negative charges. The mixtures were vortexed and incubated for 20 min at 25 °C. The resulting (siRNA–D(*l*) or siRNA–D(*c*)) were analyzed in a 20% polyacrylamide gel in TBE buffer (0.089 M Tris base, 0.089 M boric acid, 2 mM EDTA) pH 8.3. To that aim, two 0.1 nmol siRNA-containing aliquots were mixed with 1 μl of RNA loading buffer, and 1 μl of 10% SDS (w/v) was added to only one of the aliquots. The siRNA bands were stained with 1 μg/ml EtBr for 5 min and then detected by a UV transilluminator (4000, Stratagene).

A further aliquot containing 3 μg D was mixed with 1 μl of loading buffer (50%, w/v sucrose and 1%, w/v methylene blue) and run in 20% polyacrylamide gel in TBE buffer with reverse polarity. D bands were stained with Comassie Blue R-250 over night.

2.2.3. Size and zeta potential measurements

2.2.3.1. Dynamic light scattering. Samples for light scattering analyses were prepared with Tris–HCl buffer filtered across 0.02 μm to remove any trace of particulates. Size and zeta potential of siRNA–D(*l*)/(*c*) at different N/P ratios were determined by dynamic light scattering (DLS) and phase analysis light scattering (PALS), respectively, using a nanoZsizer (ZEN 3600, Malvern, UK). Additionally, size of complexes prepared with the addition of a third component to the D and siRNA mixtures was determined. To this purpose DEAE-dextran, chitosan or colominic acid were added to D solutions at 0.04:1, polymer:D molar ratio, 5 min before siRNA addition.

2.2.3.2. Transmission electron microscopy. An aliquot of siRNA-G4/G7(*l*) at N/P ratio of 10 was dropped on a standard carbon-coated cooper TEM grid, excess of liquid was removed by a tissue paper and the grids were stained with uranyl acetate (2%, w/v in water, pH 4.5) for 20 s. Imaging was performed immediately after air-drying using a TEM Phillips 301.

2.2.3.3. Atomic force microscopy. An aliquot of G4, G7 and siRNA-G4/G7(*l*) at N/P ratio of 10 was dropped on freshly cleaved mica surfaces and then air-dried at room temperature. The samples were

examined with a NanoScope IIIa - Quadrex de Di-Veeco using tapping mode under atmosphere of N_2 to minimize humidity. Probe with a spring constant of 40 N/m, resonant frequency of 300 kHz and a tip radius smaller than 10 nm were used for tapping scans (NanoDevices, MPP-11100). Image analysis was performed with WSxM software (Horcas et al., 2007).

2.3. Protection of siRNA

0.3 nmol siRNA as: siRNA–D(*l*)/(*c*) at N/P ratio of 10; siRNA–Lipofectamine2000™ complex – prepared according to manufacturer instructions – and naked siRNA, was incubated with 90 μg of RNAse A at 37 °C. At the indicated time points, an aliquot of 0.07 nmol of siRNA was mixed with RNA loading buffer containing 1 μl of 10% SDS (w/v) and immediately stored at −20 °C. siRNA's integrity was revealed by electrophoresis in 20% polyacrylamide gel, as stated in Section 2.2.2. Band intensities were analyzed with Image-Pro Plus software (Media Cybernetics, Silver Spring, MD, USA) and degree of siRNA degradation expressed as percentage was calculated as follows: siRNA degradation (%) = $100 - (I_{obs} \times 100/I_0)$, where I_{obs} is band intensity of siRNA upon RNase incubation at the time point and I_0 is the band intensity of siRNA at 0 min of incubation.

2.4. Cytotoxicity

Cell viability upon treatment with siRNA–D, measured as mitochondrial succinate dehydrogenase activity employing a tetrazolium salt (MTT) and as lactate dehydrogenase (LDH) leakage in culture supernatants, was determined on human glioblastoma cell line T98G and on the murine macrophage-like cell line J-774.

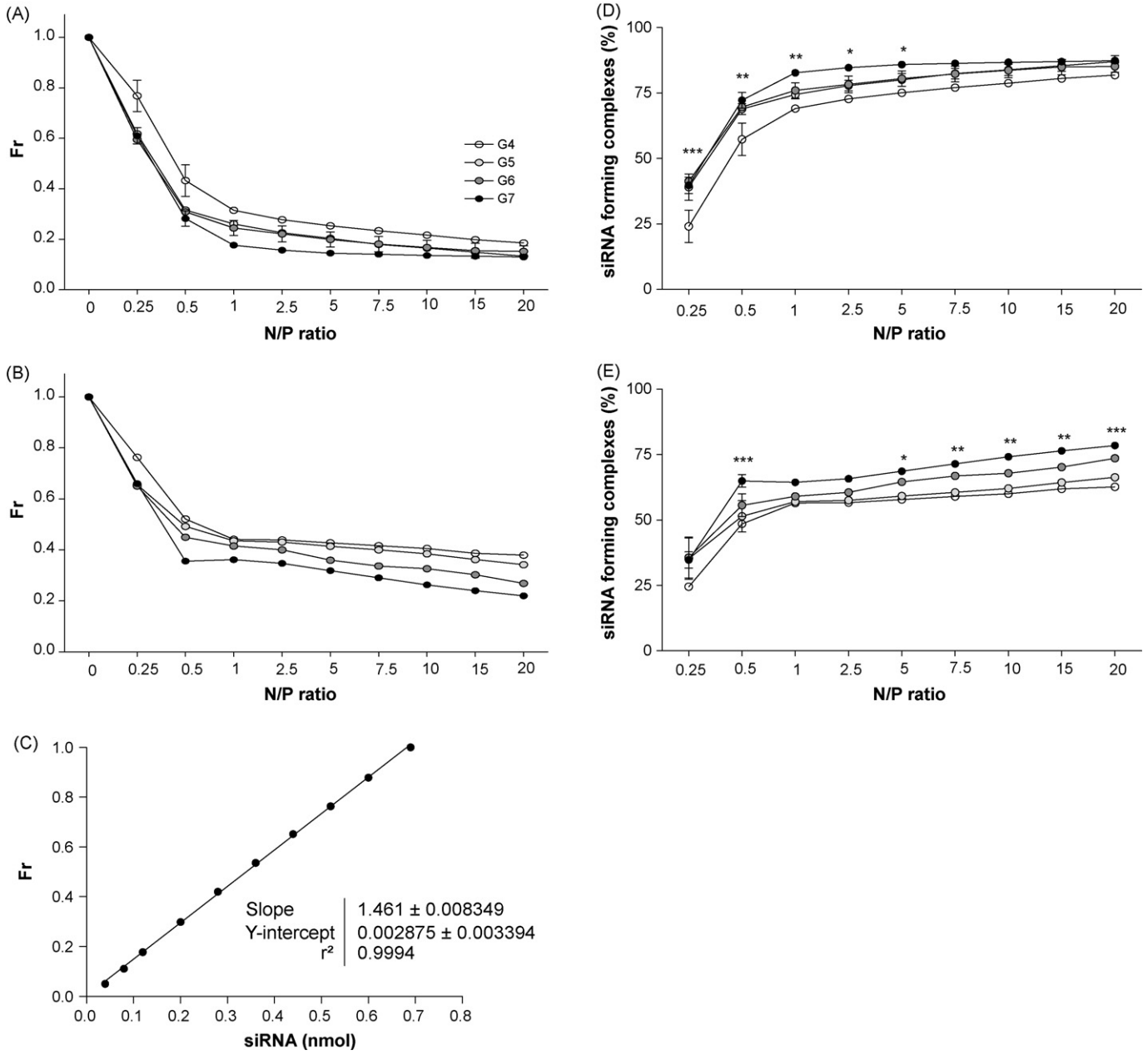

Fig. 1. EtBr displacement from siRNA by dendrimers. (A and B) F_r is reported as function of N/P ratio in 150 mM NaCl (*l*) or (*c*) medium, respectively. (C) Plot of F_r as a function of growing quantities of siRNA. (D and E) Percentage of siRNA in the complexes reported as function of N/P ratio in 150 mM (*l*) or (*c*) medium, respectively. Each data point represents the mean ± standard deviation ($n = 3$). Two-way ANOVA was used to compare statistical significance differences $^{***}p < 0.001$; $^{**}p < 0.01$; $^{*}p < 0.05$, G4 vs. G7.

Cells were routinely cultured at 37 °C in MEM supplemented with 10% (v/v) foetal calf serum (FCS), 1% (v/v) antibiotic/antimycotic (penicillin 10,000 U/ml, streptomycin sulphate 10 mg/ml, amphotericin B 25 μg/ml) and 2 mM glutamine, in 5% CO_2 and 95% humidity.

T98G and J-774 cells were seeded at a density of 5×10^4 cells/well in three 96-well flat bottom microplates and grown for 24 h at 37 °C. Medium of two plates were replaced by 100 μl of fresh MEM with 5% FCS and 50 μl of siRNA–D(*l*)/(*c*) at N/P ratio of 10 were added at a final concentration of 50 nM siRNA. One plate was incubated for 5 h and the other for 24 h at 37 °C. Medium of the third plate was replaced by 100 μl of fresh MEM without FCS, 50 μl of same siRNA–D were added and the plate was incubated for 5 h at 37 °C. After incubation, supernatants were transferred to fresh tubes, centrifuged $250 \times g$ for 4 min and LDH content was measured using lactate dehydrogenase CytoTox Kit (Promega) (Korzeniewski and Callewaert, 1983). LDH release was expressed as percentage relative to the treatment with Triton-X 100. Toxicity limit was set at 10% LDH release (Fischer et al., 2003). On the other hand, cells attached to plates were processed for MTT assay, adding 110 μl of 0.45 mg/ml MTT in medium. After 3 h incubation, MTT solution was removed, the insoluble formazan crystals were dissolved with 100 μl of dimethylsulfoxide (DMSO) and absorbance was measured at 570 nm using a microplate reader (Dynex Technologies, MRX tc). Viability of cells was express as percentage of the viability of cells grown in medium.

2.5. Confocal microscopy

T98G and J-774 cells were seeded in 24-well plates with rounded coverslips on the bottom. Upon 48 h incubation at 37 °C, the medium was removed and replaced with fresh MEM containing 50 nM of naked Cy3-labeled siRNA or Cy3-labeled siRNA-G4/G7(*l*)/(*c*) at N/P ratio of 10. Upon 5 h incubation at 37 °C, cells were washed with phosphate-buffer saline (pH 7.4) (PBS), fixed with methanol for 10 min and the emission of Cy3 was monitored with a confocal laser microscopy Olympus FV300 with a HeNe 543 nm laser. Images intensity was analyzed with Image-Pro Plus software.

2.6. siRNA transfection

2.6.1. Green fluorescence protein stably transformed cells

T98G cells constitutively expressing enhanced green fluorescent protein (EGFP) (T98G-EGFP) were kindly provided, while J-774 cells EGFP stably transformed (J-774-EGFP) were obtained in our laboratory. Briefly, J-774 cells grown at 85% confluence into T25 flask were transfected with a mixture of 2.5 μg of pEGFP-C1 plasmid and 25 μg of Lipofectamine2000™ in serum and antibiotics free MEM. After 5 h incubation at 37 °C, medium was replaced by fresh MEM with 10% FCS and cells continued growing for 5 days. Then, stably transformed cells were selected by treatment with G418, first cells were grown with 200 μg/ml G418 for 3 days and concentration was subsequently increased in 100 μg/ml every third day up to 700 μg/ml. Finally, both J-774-EGFP and T98G-EGFP cells were maintained in MEM containing 500 μg/ml G418. EGFP expression was evaluated by flow cytometry. Briefly, cells were harvested by trypsinization, washed two times with PBS and fixed in 1% formaldehyde solution at 4 °C for at least 2 h. Cells were washed and suspended in PBS, and then a total of 10,000 cells were introduced into a FACSCalibur flow cytometer (Becton Dickinson, San Jose, CA, USA). Data was analyzed using WinMDI 2.9 software. The inhibition of EGFP expression was carried out with at least 90% of cell expressing EGFP.

2.6.2. Inhibition of EGFP expression

T98G-EGFP and J-774-EGFP cells were seeded at a density of 1.2×10^5 cells/well in 6-well plates in MEM containing 500 μg/ml G418 and 10% of FCS. After 24 h, the culture medium was replaced by 1.2 ml of serum and antibiotics free MEM, and 50 μl of siRNA–D(*l*)/(*c*) at N/P ratio of 10 or siRNA-Lipofectamine2000™ complex were added at a final concentration of 50 nM siRNA per well. After 5 h incubation at 37 °C, the culture medium was replaced with fresh MEM containing 5% FCS. After 72 h, cells were prepared for flow cytometry analyses as described above and data from at

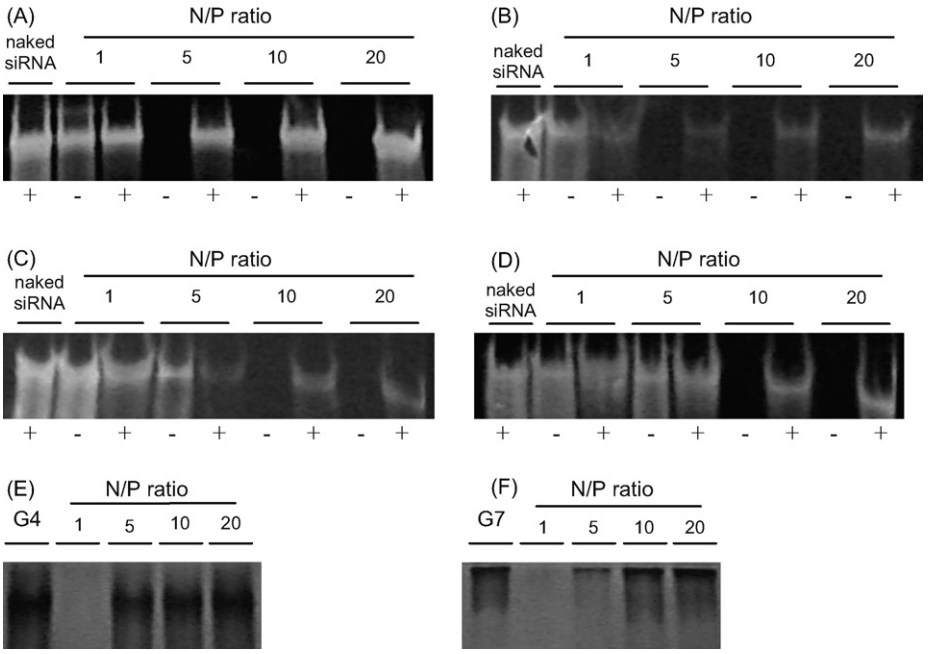

Fig. 2. Polyacrylamide gel electrophoresis of naked siRNA and (A) siRNA-G4, (B) siRNA-G5, (C) siRNA-G6 and (D) siRNA-G7 as function of N/P ratio; each siRNA–D was treated with (+) or without (−) 1% SDS (w/v). (E and F) Reverse polarity polyacrylamide gel electrophoresis of siRNA-G4 siRNA-G7, respectively. N/P ratio of 5 corresponded to a D: siRNA mol ratio of 4.5 and 2, for G4 and G5, respectively, while N/P ratio of 10 corresponded to 2 and 1 mol ratio, for G6 and G7, respectively.

least 50,000 cells were acquired. Inhibition of EGFP expression was calculated using the geometric mean (Gm) and express as percentage as follows: EGFP inhibition (%) = $100 - ((Gm_{obs}/Gm_c) \times 100)$, where Gm_{obs} is the Gm of cells after treatment, and Gm_c is the Gm of cells grown in medium.

2.7. Statistical analysis

Statistical analyses were performed by Student's *t*-test or two-way ANOVA followed by Bonferroni's test using Prisma 4.00 software (Graphpad Software Corporation, San Diego, CA, USA), and significance levels are indicated in the figure legends.

3. Results

3.1. Analysis of siRNA–D formation and characterization

3.1.1. Ethidium bromide displacement assay

Formation of siRNA–D was studied by determining the relative fluorescence (F_r) of EtBr intercalated in siRNA, as function of D addition (referred as N/P ratio) in (*l*) or (*c*) media. The electrostatic interactions of cationic ammonium groups on D surface with negatively charged phosphate groups on siRNA backbone (Zhou et al., 2006), responsible for the displacement of the intercalating EtBr from siRNA, lead to a diminution of EtBr fluorescence.

As the N/P ratio was increased, an exponential decay of F_r was recorded: low quantities of D caused a pronounced drop of F_r, which remained almost unchanged upon further D addition (Fig. 1). In (*l*) medium, F_r dropped up to N/P ratio of 1 (Fig. 1A), whereas in (*c*) medium F_r dropped less pronouncedly and ceased at N/P ratio of 0.5 (Fig. 1B).

On the other hand, the linear regression from the plot of F_r vs. added siRNA (Fig. 1C) was used to quantify free siRNA remaining in the complexes after each D addition.

Next, the percentage of siRNA forming complexes with D was calculated as follows: $[0.69 - (F_r - 0.002875)/1.46] \times 100/0.69$, where 0.69 nmol was the total siRNA amount, and 0.002875 and 1.646 was the Y-intercept and the slope of the linear regression of the F_r vs. siRNA curve, respectively.

It was observed that NaCl strongly influenced the electrostatic interaction between siRNA and D. In NaCl lacking medium, and up to N/P ratio of 1, between 70 and 83% of siRNA formed complexes with G4 and G7 D, respectively (Fig. 1D). From that on, the amount of siRNA involved in complexes was slightly increased to reach a maximum of 90% for all D at the N/P ratio of 20. In NaCl containing medium on the other hand, and up to N/P ratio of 0.5, between 50 and 60% of siRNA formed complexes with G4 and G7 D, respectively (Fig. 1E). From that on, the amount of siRNA in complexes was increased to reach a maximum of 60 and 80% for G4 and G7 D, respectively, at N/P ratio of 20.

The displacement of EtBr showed that all D formed complexes with siRNA. The largest D produced highest EtBr displacement and in NaCl containing medium, a lower EtBr displacement was produced; in other words, lower quantities of siRNA formed complexes with D.

3.1.2. Polyacrylamide gel electrophoresis retardation

Both G4 and G5 D retarded siRNA at N/P ratio ≥5 (Fig. 2A and B), while G6 and G7 D completely retarded siRNA at N/P ratio ≥10

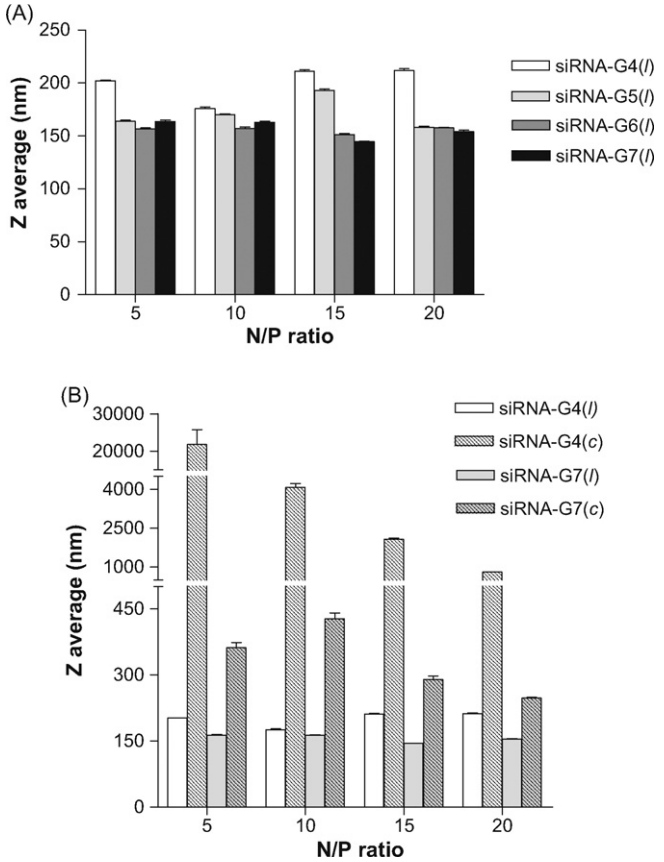

Fig. 3. Hydrodynamic size determined by DLS of (A) siRNA–D as function of N/P ratio in (*l*) medium, and (B) of siRNA-G4/G7 in NaCl (*l*) or (*c*) medium.

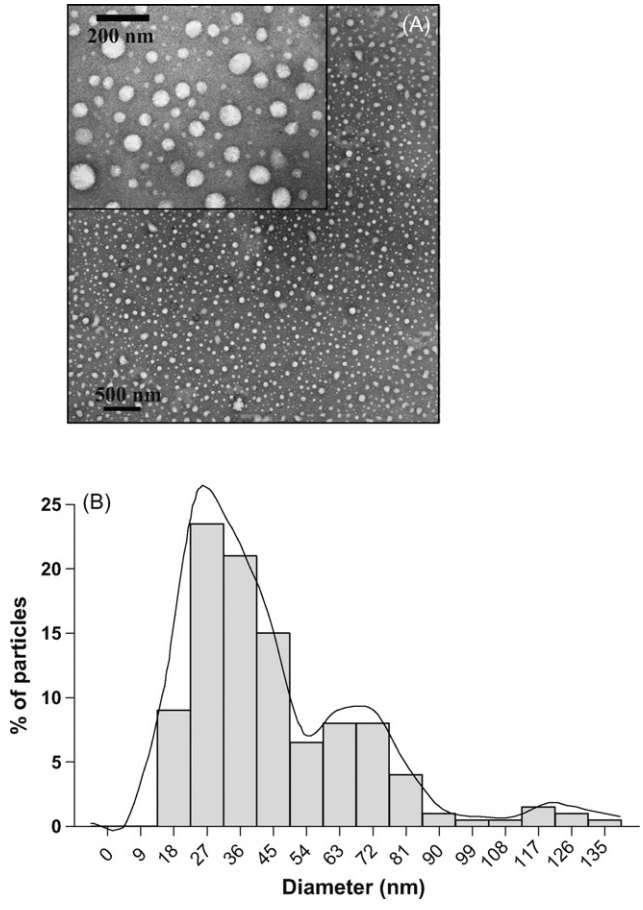

Fig. 4. (A) Transmission electron microscopy image of siRNA-G7(*l*) at N/P ratio of 10. Inset: detailed picture at higher magnification. (B) Distribution of particle diameters derived from image (A).

(Fig. 2C and D). This indicated that at low N/P ratios, the smaller D was more efficient to establish ionic interactions with siRNA than the largest ones. As shown in Fig. 2, complexes were disrupted by strong ionic detergent such as SDS. No differences were observed between siRNA retardation of complexes prepared in (*l*) or (*c*) media.

On the other hand, when N/P ratio was ≥5 (G4, G5) and ≥10 (G6, G7), the presence of free D was revealed by reverse polarity gel electrophoresis (Fig. 2E and F). This indicated that beyond those ratios, a mixture of free D and siRNA–D can be found.

3.1.3. Size

3.1.3.1. Dynamic light scattering. Independently on D size and N/P ratio, the hydrodynamic diameters of siRNA–D(*l*) were between 150 and 200 nm, with low polydipersity (Pdi 0.05–0.1) (Fig. 3A). Opposing, the hydrodynamic diameters of siRNA–D(*c*) were bigger than the formers and strongly dependent on D size and N/P ratio. For instance as N/P ratio was increased, the size of siRNA-G4(*c*) and siRNA-G7(*c*) decreased from several μm to 800 nm, and from 450 to 250 nm, respectively (Fig. 3B).

Kukowska-Lantallo in 1996, showed that transfection efficiency was increased as the size of the pDNA–D was decreased upon DEAE-dextran addition (Kukowska-Latallo et al., 1996). Therefore, aiming to reduce the size of siRNA–D, the effect of cationic polymers (DEAE-dextran at pH 7.4 and chitosan at pH 4.5) and the anionic polymer colominic acid (at pH 7.4) on the size of the siRNA–D was determined. However, we found that neither the cationic nor the anionic polymers added to siRNA–D in (*l*) or (*c*) media was capable of decreasing their size.

3.1.3.2. Transmission electron microscopy (TEM). The image analysis of siRNA-G4/G7(*l*) showed spherical structures with three different media size (Fig. 4A), being the biggest proportion small complexes in the range of 30–45 nm, followed by intermediate range complexes of 60–80 nm and a smallest proportion of large complexes of around 130 nm (Fig. 4B).

3.1.3.3. Atomic force microscopy (AFM). G4 D formed a film with some prominent spherical structures of 15 nm on the mica surface (Fig. 5A), while siRNA-G4(*l*) formed isolated spherical structures of 16 and 30 nm (Fig. 5B). On the other hand, G7 D formed randomly deposited globular structures (Fig. 5C) (similar to those reported by Li et al. (2000) for G4 at 0.1%, w/w, Li et al., 2000), while siRNA-G7(*l*) formed individual structures of 15 and 45 nm (Fig. 5D).

The 15/16 nm structures could represent free D revealed by reverse polarity electrophoresis (see Section 3.1.2) and reported by Li et al. (2000), while the 30/45 nm structures could represent the abundant but small complexes revealed by TEM. These coincident microscopic observations were different from DLS measurements that showed bigger structures of 150–200 nm. In our case, we have considered that both AFM and TEM were the two techniques that most accurately determined the size of siRNA–D: 30–45 nm, 60–80 nm and 130 nm. Our assumption was based in the findings from Hoo et al. (2008), who demonstrated that two mixtures of 20 nm and 100 nm polystyrene nanoparticles at 5:1 and 8:1 ratios, are shown by AFM as two populations of 16 and 98 nm nanoparticles composing each mixture, while DLS yields only one population of 109 nm or 245 nm for each mixture, respectively (Hoo et al., 2008). Additionally, also Hobel et al. (2008) had reported

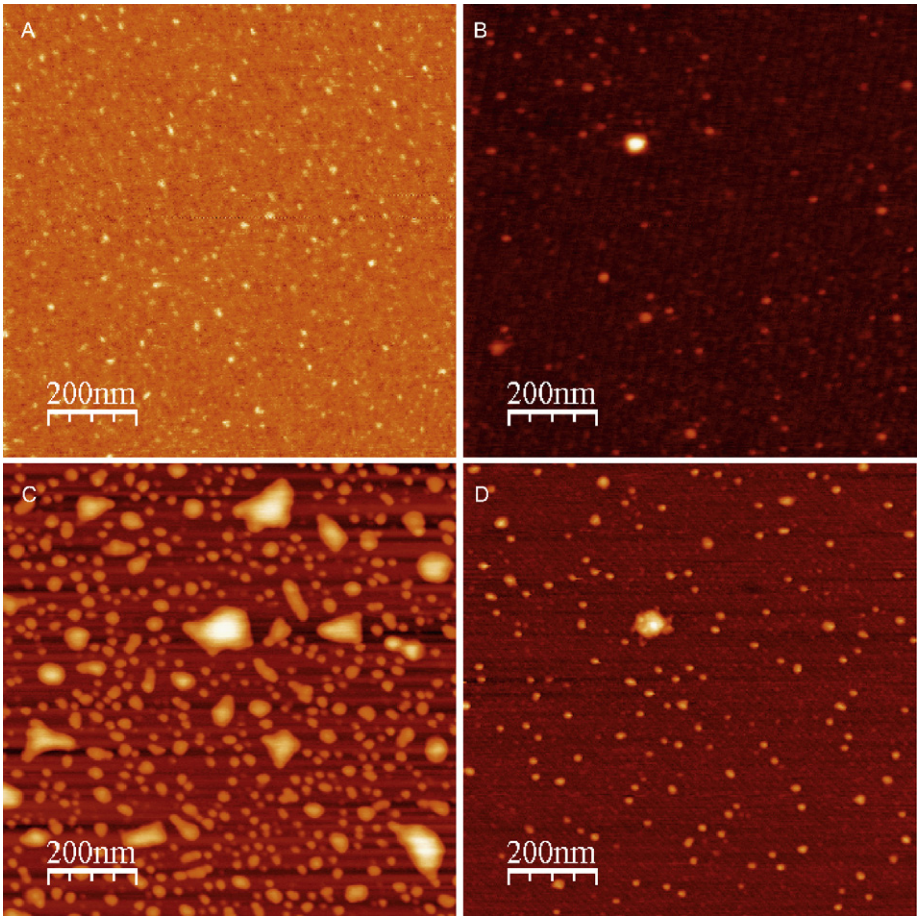

Fig. 5. AFM images of (A) G4, (B) siRNA-G4(*l*), (C) G7 and (D) siRNA-G7(*l*). Same amount of both free D and complexes at N/P ratio of 10 were deposited on mica (0.09 μg D and 0.001 μmol of siRNA).

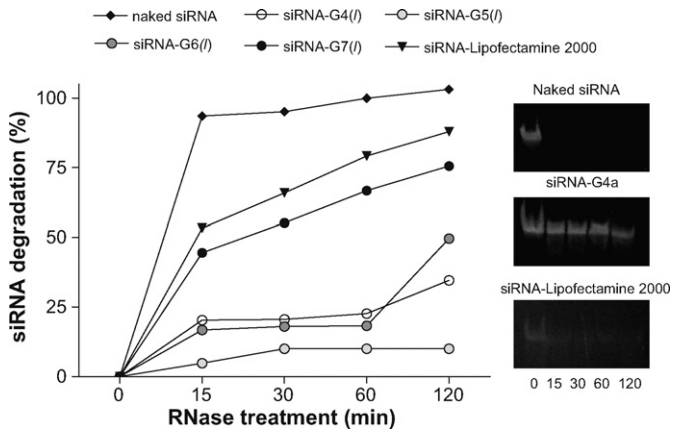

Fig. 6. Protection of siRNA upon RNAse treatment. Samples were run in 20% polyacrylamide gel electrophoresis, gel bands intensity (see insert) were analyzed and siRNA degradation was calculated at each time point.

two populations of 25–75 and 60–130 nm for PEI F25-LMW/DNA complexes by AFM, while using DLS only structures of several hundred nm were reported (Hobel et al., 2008). These findings indicated that size measurement of heterogeneously sized polymer complexes in the sub-micron range must be faced by different and complementary analytical tools.

3.1.4. Zeta potential

The zeta potential of D was decreased from +35–45 mV to +15 mV in the presence of NaCl. On the other hand, zeta potential of siRNA remained constant at −20 to 25 mV independently of the ionic strength. Zeta potential of siRNA–D(*l*) were nearly +25 mV and was independent of the N/P ratio; likewise zeta potential of siRNA–D(*c*) were close to zero.

3.1.5. Protection of siRNA

Stability of siRNA molecules upon forming complexes with D was analyzed in the presence of RNase A by gel electrophoresis. It was found that siRNA–D protected the siRNA in variable degree, as shown by intensity band analysis upon gel electrophoresis (Fig. 6). It was observed that naked siRNA was completely degraded upon 15 min incubation with RNase A. Less than 20% of siRNA-G4/G5/G6, while 65 and 80% of siRNA-G7/Lipofectamine2000™, respectively, was degraded after 60 min.

3.2. Cytotoxicity

The toxicity of siRNA–D at N/P ratio of 10 was evaluated in T98G and J-774 cells at 50 nM siRNA. None of the siRNA–D(*l*)/(*c*) reduced the viability of both cell types, as measured by MTT assay or by LDH leakage, neither upon 5 h nor 24 h incubation in medium with FCS (Fig. 7A–D). When incubated in medium without FCS along 5 h (same conditions as for inhibition of EGFP expression), none of the siRNA–D(*l*)/(*c*) reduced the viability of J-774 cells. On the other hand, the viability of T98G cells was slightly reduced (10%) upon incubation with siRNA-G5/G6/G7(*l*) as measured by MTT assay, but no significant LDH leakage was registered (Fig. 7B and D).

3.3. Cellular uptake of siRNA

Cy3-labeled siRNA (siRNA-Cy3) was used to evaluate if complex formation could increase the siRNA uptake by phagocytic (J-774) and non-phagocytic cells (T98G), and to search for differences between the uptake of complexes prepared in (*l*) or (*c*) media. It was found that, while naked siRNA-Cy3 did not enter the cells after

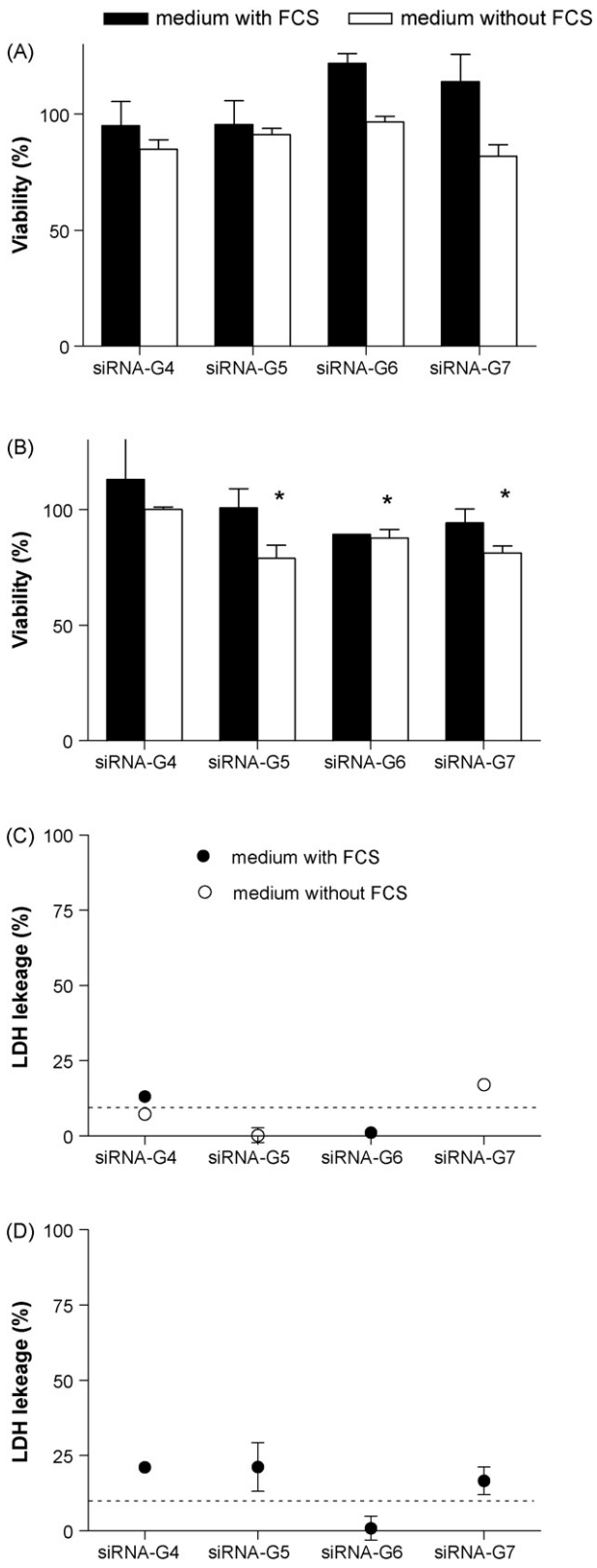

Fig. 7. Viability of (A) J-774 and (B) T98G cells as measured by MTT assay and LDH leakage (C) and (D), respectively, upon 24 h (in medium with FCS) or 5 h (in medium without FCS), incubation with siRNA–D at N/P ratio of 10. Concentration of siRNA in each well was 50 nM. Each data point represents the mean ± standard deviation ($n = 5$). Two-way ANOVA was used to compare statistical significance differences of treatments, $^{*}p < 0.05$ siRNA–D vs. control cells.

5 h incubation, as judged by the absence of fluorescence (Fig. 8E and K), all siRNA-Cy3-G4/G7(*l*)/(*c*) were internalized in different degree (Fig. 8), as shown by red fluorescent points in cytoplasm (Fig. 8, insets). Fluorescence intensity analysis showed that siRNA-Cy3-G7 uptake was between 3 and 6 folds higher than that of siRNA-Cy3-G4, being highest the uptake of siRNA-Cy3-D(*l*) (Fig. 8F and L). Overall, T98G cells internalized between 2 and 3 folds more siRNA–D than J-774 cells. On T98G cells, the uptake of siRNA-Cy3-D(*l*) was higher than that of siRNA-Cy3-D(*c*). Finally on J-774 cells, the uptake of siRNA-Cy3-G4(*l*) was 2 folds higher than that of siRNA-Cy3-G4(*c*), whereas the uptake of siRNA-Cy3-G7 remained independent of the presence of NaCl.

3.4. Inhibition of EGFP expression

Similar to Lipofectamine2000 we found that the inhibition of EGFP expression by siRNA–D was depended on the cell type, and also was different according if siRNA–D(*l*) or siRNA–D(*c*) was used.

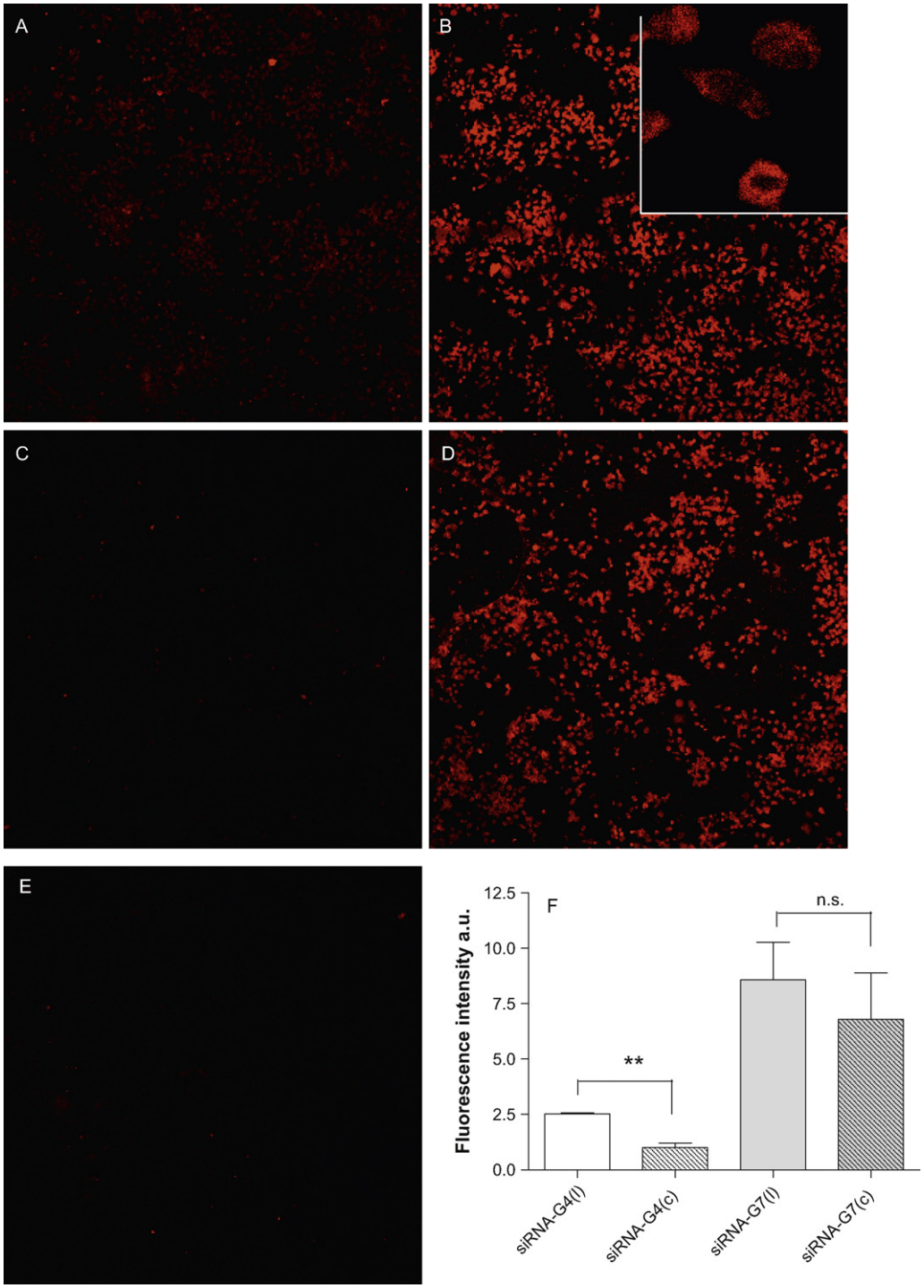

Fig. 8. Confocal fluorescence microscopic images of J-774 (A–E) and T98G cells (G–K) upon 5 h incubation with siRNA-Cy3-G4(*l*) (A and G), siRNA-Cy3-G7(*l*) (B and H), siRNA-Cy3-G4(*c*) (C and I), siRNA-Cy3-G7(*c*) (D and J) or naked siRNA-Cy3 (E and K), all pictures were taken at 10×. Insets: detailed images taken at 60×. (F and L) Fluorescence intensity analysis. Student's *t*-test was used to compared statistical significance differences of treatments, $^{**}p < 0.01$; $^{*}p < 0.05$; n.s. not significant.

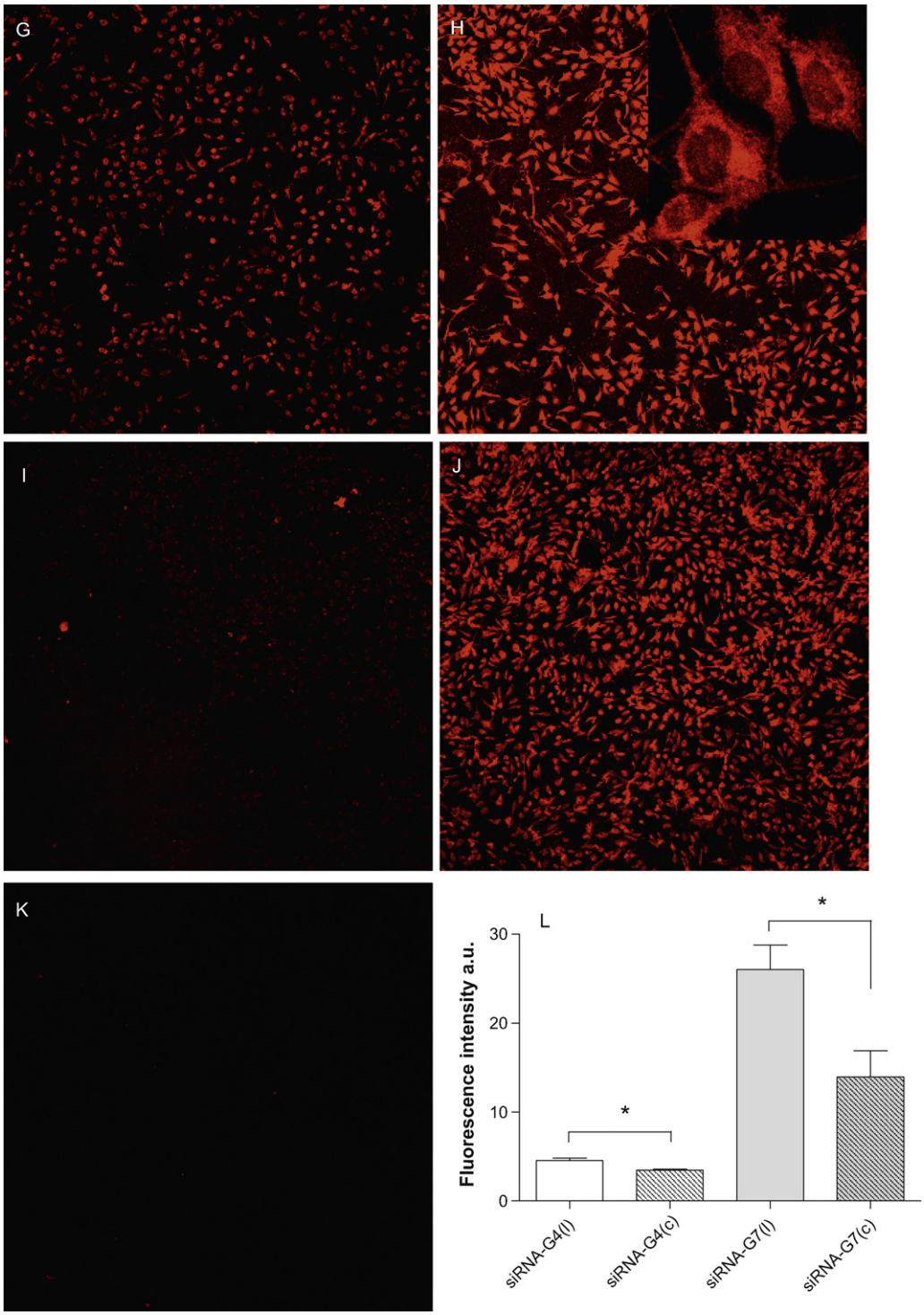

Fig. 8. (*Continued*).

siRNA–D(*c*) produced null or weak (12%) inhibition of EGFP expression on T98G-EGFP and J-774-EGFP cells. On the other hand, the inhibition produced on both cell types by siRNA–D(*l*), was D-size dependent (Fig. 9A). siRNA-G7(*l*) produced the highest level of inhibition on T98G-EGFP (35%) and J-774-EGFP (45%) cells, while Lipofectamine2000 produced 70 and 40% inhibition in both cell types, respectively. It is worth to note that in J-774 cells, siRNA-G7(*l*) produced the same EGFP gene silencing than Lipofectamine2000.

To test the effect of FCS on the activity of siRNA–D(*l*), treatments were performed at 5 and 20% FCS. The activity of siRNA-G7(*l*) and Lipofectamine2000 in 5% FCS, were not significantly different to those in the absence of FCS. However, the activity of siRNA-G7(*l*) or Lipofectamine2000 in 20% FCS were significantly decreased on both cell types, to half of those in the absence of FCS (Fig. 9B). Finally, it was observed that the activity of siRNA-G4(*l*) on T98G-EGFP cell in 20% FCS was slightly increased as compared to that in the absence of FCS.

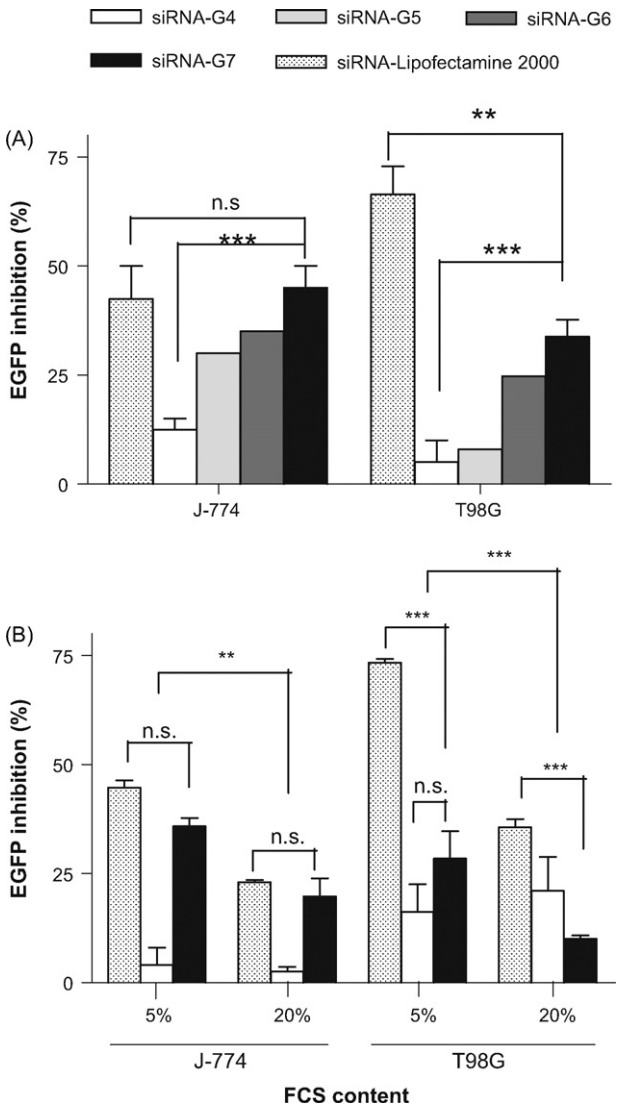

Fig. 9. Inhibition of EGFP expression upon 5 h treatment with siRNA–D at N/P ration of 10, as function of D generation and cell type, (A) in the absence of FCS and (B) in 5 or 20% FCS. siRNA–Lipofectamine2000 complex was used as positive control. Concentration of siRNA in each well was 50 nM. Each data point represents the mean ± standard deviation ($n = 5$). Two-way ANOVA was used to compare statistical significance differences of treatments, $^{***}p < 0.001$; $^{**}p < 0.01$; n.s. not significant.

4. Discussion and conclusions

The first attempt on using D as delivery systems for siRNA was in 2005, where PAMAM G5 D were used to prepare siRNA–D that were covalently conjugated to Tat cell penetrating peptide and to the fluorescent dye BODIPY, in order to inhibit the MDR1 gene expression on NIH 3T3 cells (Kang et al., 2005). That siRNA–D produced only 10% inhibition of MDR1 expression, against 70% obtained with Lipofectamine2000. Increased D concentrations up to 30 μg/ml raised the inhibition up to 35%, but the toxicity was also increased to unacceptable levels. Such limited biological activity was attributed to the EDA core PAMAM backbones, that were responsible for an incomplete release of siRNA into the cells and it was finally concluded that EDA core PAMAM dendrimers were not suitable agents for siRNA delivery.

Previous data indicated the existence of a direct relationship between D flexibility and transfection efficiency, demonstrated for pDNA–degraded D complexes (Tang et al., 1996). Therefore, the next steps were directed towards the synthesis of D with the new core triethanolamine (TEA) (Zhou et al., 2006). TEA core D start their branching units at 10 successive bonds from the amine center, which generates a more flexible structure with less densely packed branching units and end groups, than commercially available NH_3 or EDA core D. In theory, TEA core D (TEA D) should exhibit the same increased flexibility than degraded dendrimers. siRNA-G7 TEA D at 50 nM siRNA, caused 50% inhibition of luciferase expression while maintaining 80% cell viability in A549Luc cells expressing the GL3 luciferase gene. However, although 80% of inhibition was achieved at 100 nM siRNA, this was accompanied by a reduction of 50% in cell viability. Transfection controls with commercial products were absent (Zhou et al., 2006).

On the other hand, it is well documented that the size of pDNA–D can be controlled either by using partially degraded (flexible) D (Tang and Szoka, 1997) or by including small anionic molecules such as sulphate dextran or DNA oligomers (Kukowska-Latallo et al., 1996; Maksimenko et al., 2003). Both strategies render more homogeneous population of smaller particles which also display increased transfection efficiency. Recently it has also been reported that siRNA–polyethylenimine (PEI) complexes greater than 150 nm were unable to mediate gene silencing *in vitro* (Grayson et al., 2006).

This last result notwithstanding, beyond raising questions on whether or not D flexibility is the unique requirement for silencing activity, it also supports the fact that the small size of siRNA-TEA D used by Zhou et al. (2006) could be a true key factor for their silencing activity. In this light, the revision of the poor results obtained by Kang et al. (2005) could be ascribed to the existence of heterogeneously sized and aggregated complexes. In other words, the low activity could be owed to large complexes resultant from the sticky hydrophobic moieties attached to the D, and not exclusively to an incomplete intracellular release of the siRNA, that could be overcame if D flexibility were increased.

Finally, since electrostatic repulsion and Z potential are both decreased in high ionic strength media (Hunter, 1988), it is also possible to state that the charge screening produced by high ionic strength on electrostatic complexes could also difficult their compactation, being also responsible for their aggregation.

Up to the moment, the influence on size and on silencing activity of electrostatic-driven complexes has only been screened for interactions between pDNA and D, here we have surveyed the influence of the ionic strength on the size, inter-polymer interactions, uptake and silencing activity of siRNA and “not flexible” EDA core PAMAM D complexes.

First, the electrophoretic retardation study showed that in order to complexate the whole available siRNA molecules, a minimum N/P ratio of 5 (for G4, G5) and 10 (for G6, G7), was required. This assay revealed that structurally stable complexes could be formed, independently of the ionic strength of the preparation media.

Secondly, the EtBr displacement study showed the relative binding affinity between D and siRNA was dependent on D size and N/P ratio, and also on the ionic strength of the preparation media. In lacking NaCl media and at low N/P ratio (<5), the largest D produced the highest EtBr displacement, suggesting that the interaction between siRNA and D occurred with higher relative binding affinity. These results are coincident with previous findings on biophysical characterization of pDNA–D complexes (Kukowska-Latallo et al., 1996; Tang and Szoka, 1997; Braun et al., 2005; Fant et al., 2008), where a primarily electrostatic interaction between pDNA–D was reported, that showed to be decreased at higher ionic strength due to screening effects.

In third place, three different independent techniques (DLS, TEM and AFM) were employed to estimate the size of the complexes. In general terms, we found an inverse dependence between the size and the binding affinity, and between the size and the ionic strength of preparation media. The size of the complexes prepared in NaCl lacking media and showing highest affinity was <200 nm, while the size of complexes prepared in NaCl containing media showed

lower affinity and ranged in the order of several hundred nm to μm. Finally, we observed that the *Z* potential of small siRNA–D was reduced from +25 mV to 0 when NaCl was added to the medium, this drop being accompanied by the formation of largest complexes or even aggregates.

In sum, those findings indicated that the ionic strength of the media was a main determinant of the size of siRNA–D, being therefore the ultimate responsible for the inhibition of EGFP expression (silencing activity): complexes prepared in NaCl containing media were slightly active on phagocytic and inactive on non-phagocytic cells, while the smaller complexes prepared in lacking NaCl media exhibited the highest silencing activity.

If well G7 D presented a high binding affinity for siRNA, we observed that siRNA-G7 neither protected the siRNA from enzymatic degradation nor impaired the detachment of some siRNA molecules when the complex was submitted to electrophoresis. As compared to that formed with G7, siRNA-G4 was much more stable against RNase A, also impairing the electrophoretic detachment of siRNA. However, while siRNA-G4 was inactive, both uptake and silencing was maximal for siRNA-G7 in the two cell lines, indicating that structural constraints specific for siRNA-G7 and other than size could account for its silencing activity.

Finally, we observed that in 5% serum both siRNA-G7 and siRNA–Lipofectamine2000 silencing activity remained at the same level than in the absence of serum, decreasing to the half when in 20% serum. Opposite, in 20% serum siRNA-G4 complex increased the silencing activity up to maximal values of 20% on T98G cells.

These results confirmed that modifying the chemical structure of D was not the only way of achieving siRNA–D suitable for silencing activity. Our results were in agreement with recent studies where longer RNA, higher G D and higher N/P ratio rendered stable and uniformly distributed complexes sized in the nanoscale (60–110 nm) (Shen et al., 2007). Large complexes in the range of micrometers could hardly be pinocitosed or phagocitosed by cells; being the uptake the obligate step prior to the cytoplasmic delivery of siRNA, small sized complexes resulting from decreasing the ionic strength of the media were in fact the true responsible for an efficient silencing.

Additionally, there is growing experimental evidence supporting the fact that the electrostatic interaction between nucleic acids and its cationic carrier plays a crucial role in the unpacking step needed to release free siRNA molecules in cytoplasm. Briefly, for a given length of DNA, the cationic polymers of highest molecular weight are known to strongly bind to DNA than those smaller (Abdallah et al., 1996; Plank et al., 1999; Schaffer et al., 2000). This strong interaction is responsible for unpacking and difficult the release of DNA. Up to date, there is no available data on siRNA–D interactions (Gary et al., 2007) and beyond their small size needed for internalization, structural constraints of complexes prepared with largest D seemed to be required for an effective silencing.

Acknowledgements

This research was supported by grants from Secretaría de Investigaciones, Universidad Nacional de Quilmes and Comisión de Investigaciones Cientificas, Prov. Bs. As. (CIC). M.J. Morilla and E.L. Romero are members of the Carrera del Investigador Científico del Consejo Nacional de Investigaciones Científicas y Técnicas (CONICET, Argentina). A.P. Perez has got a fellowship from CONICET, Argentina.

References

Abdallah, B., Hassan, A., Benoist, C., Goula, D., Behr, J.P., Demeneix, B.A., 1996. A powerful nonviral vector for in vivo gene transfer into the adult mammalian brain: polyethylenimine. Hum. Gene Ther. 7, 1947–1954.

Bielinska, A., Kukowska-Latallo, J.F., Johnson, J., Tomalia, D.A., Baker Jr., J.R., 1996. Regulation of in vitro gene expression using antisense oligonucleotides or antisense expression plasmids transfected using starburst PAMAM dendrimers. Nucleic Acids Res. 24, 2176–2182.

Braun, C.S., Vetro, J.A., Tomalia, D.A., Koe, G.S., Koe, J.G., Middaugh, C.R., 2005. Structure/function relationships of polyamidoamine/DNA dendrimers as gene delivery vehicles. J. Pharm. Sci. 94, 423–436.

Devi, G.R., 2006. siRNA-based approaches in cancer therapy. Cancer Gene. Ther. 13, 819–829.

Dufes, C., Uchegbu, I.F., Schatzlein, A.G., 2005. Dendrimers in gene delivery. Adv. Drug Deliv. Rev. 57, 2177–2202.

Dung, T.H., Kim, J.S., Juliano, R.L., Yoo, H., 2008. Preparation and evaluation of cholesteryl PAMAM dendrimers as nano delivery agents for antisense oligonucleotides. Colloids Surf. A: Physicochem. Eng. Aspects 313, 273–377.

Eccleston, A., Eggleston, A.K., 2004. Introduction RNA interference. Nature 431, 337.

Elbashir, S.M., Harborth, J., Lendeckel, W., Yalcin, A., Weber, K., Tuschl, T., 2001. Duplex of 21-nucleotide RNAs mediate RNA interference in cultured mammalian cells. Nature 411, 494–498.

Fant, K., Esbjorner, E.K., Lincoln, P., Norden, B., 2008. DNA condensation by PAMAM dendrimers: self-assembly characteristics and effect on transcription. Biochemistry 47, 1732–1740.

Fattal, E., Bochot, A., 2008. State of the art and perspectives for the delivery of antisense oligonucleotides and siRNA by polymeric nanocarriers. Int. J. Pharm. 364, 237–248.

Fischer, D., Li, Y., Ahlemeyer, B., Krieglstein, J., Kissel, T., 2003. In vitro cytotoxicity testing of polycations: influence of polymer structure on cell viability and hemolysis. Biomaterials 24, 1121–1131.

Gary, D.J., Puri, N., Won, Y.Y., 2007. Polymer-based siRNA delivery: perspectives on the fundamental and phenomenological distinctions from polymer-based DNA delivery. J. Control. Release 121, 64–73.

Grayson, A.C.R., Doody, A.M., Putnam, D., 2006. Biophysical and structural characterization of polyethylenimine-mediated siRNA delivery in vitro. Pharm. Res. 28, 1868–1876.

Haensler, J., Szoka, F.C.J., 1993. Polyamidoamine cascade polymers mediate efficient transfection of cells in culture. Bioconjug. Chem. 4, 372–379.

Hobel, S., Prinz, R., Malek, A., Urban-Klein, B., Sitterberg, J., Bakowsky, U., Czubayko, F., Aigner, A., 2008. Polyethylenimine PEI F25-LMW allows the long-term storage of frozen complexes as fully active reagents in siRNA-mediated gene targeting and DNA delivery. Eur. J. Pharm. Biopharm. 70, 29–41.

Hoo, C.M., Starostin, N., West, P., Mecartney, M.L., 2008. A comparison of atomic force microscopy (AFM) and dynamic light scattering (DLS) methods to characterize nanoparticle size distributions. J. Nanopart. Res. 10, 89–96.

Horcas, I., Fernandez, R., Gomez-Rodriguez, J.M., Colchero, J., Gomez-Herrero, J., Baro, A.M., 2007. WSXM: a software for scanning probe microscopy and a tool for nanotechnology. Rev. Sci. Instrum. 78, 013705.

Hunter, R.L., 1988. Zeta Potential in Colloid Science: Principles and Applications. Academic Press, UK.

Kang, H., DeLong, R., Fisher, M.H., Juliano, R.L., 2005. Tat-conjugated PAMAM dendrimers as delivery agents for antisense and siRNA oligonucleotides. Pharm. Res. 22, 2099–2106.

Korzeniewski, C., Callewaert, D.M., 1983. An enzyme-release assay for natural cytotoxicity. J. Immunol. Methods 64, 313–320.

Kukowska-Latallo, J.F., Bielinska, A.U., Johnson, J., Spindler, R., Tomalia, D.A., Baker Jr., J.R., 1996. Efficient transfer of genetic material into mammalian cells using Starburst polyamidoamine dendrimers. Proc. Natl. Acad. Sci. U.S.A. 93, 4897–4902.

Li, J., Piehler, L.T., Qin, D., Baker, J.R., Tomalia, D.A., 2000. Visualization and characterization of poly(amidoamine) dendrimers by atomic force microscopy. Langmuir 16, 5613–5616.

Maksimenko, A.V., Mandrouguine, V., Gottikh, M.B., Bertrand, J.R., Majoral, J.P., Malvy, C., 2003. Optimisation of dendrimer-mediated gene transfer by anionic oligomers. J. Gene Med. 5, 61–71.

Paroo, Z., Corey, D.R., 2004. Challenges for RNAi in vivo. Trends Biotechnol. 22, 390–394.

Plank, C., Tang, M.X., Wolfe, A.R., Szoka, F.C.J., 1999. Branched cationic peptides for gene delivery: role of type and number of cationic residues in formation and in vitro activity of DNA polyplexes. Hum. Gene Ther. 10, 319–332.

Quarck, R., Holvoet, P., 2004. Gene therapy approaches for cardiovascular diseases. Curr. Gene Ther. 4, 207–223.

Riddihough, G., 2005. In the forests of RNA dark matter. Science 309, 1507.

Schaffer, D.V., Fidelman, N.A., Dan, N., Lauffenburger, D.A., 2000. Vector unpacking as a potential barrier for receptor mediated polyplex gene delivery. Biotechnol. Bioeng. 67, 598–606.

Shen, X.C., Zhou, J., Liu, X., Wu, J., Qu, F., Zhang, Z.L., Pang, D.W., Quelever, G., Zhang, C.C., Peng, L., 2007. Importance of size-to-charge ratio in construction of stable and uniform nanoscale RNA/dendrimer complexes. Org. Biomol. Chem. 5, 3674–3681.

Sioud, M., 2005. On the delivery of small interfering RNAs into mammalian cells. Expert Opin. Drug Deliv. 2, 639–651.

Spagnou, S., Miller, A.D., Keller, M., 2004. Lipidic carriers of siRNA: differences in the formulation, cellular uptake, and delivery with plasmid DNA. Biochemistry 43, 13348–13356.

Svenson, S., Tomalia, D.A., 2005. Dendrimers in biomedical applications—reflections on the field. Adv. Drug Deliv. Rev. 57, 2106–2129.

Tang, M.X., Redemann, C.T., Szoka, F.C.J., 1996. In vitro gene delivery by degraded polyamidoamine dendrimers. Bioconjug. Chem. 7, 703–714.

Tang, M.X., Szoka, F.C., 1997. The influence of polymer structure on the interactions of cationic polymers with DNA and morphology of the resulting complexes. Gene Ther. 4, 823–832.
Yoo, H., Juliano, R.L., 2000. Enhanced delivery of antisense oligonucleotides with fluorophore-conjugated PAMAM dendrimers. Nucleic Acids Res. 28, 4225–4231.
Yoo, H., Sazani, P., Juliano, R.L., 1999. PAMAM dendrimers as delivery agents for antisense oligonucleotides. Pharm. Res. 16, 1799–1804.
Zhang, S., Zhao, B., Jiang, H., Wang, B., Ma, B., 2007. Cationic lipids and polymers mediated vectors for delivery of siRNA. J. Control. Release 123, 1–10.
Zhou, J., Wu, J., Hafdi, N., Behr, J.P., Erbacher, P., Peng, L., 2006. PAMAM dendrimers for efficient siRNA delivery and potent gene silencing. Chem. Commun. (Camb.), 2362–2364.